PHYSICAL REVIEW B **73**, 041404(R) (2006)

Mapping the electron correlation in two-electron photoemission

F. O. Schumann, C. Winkler, G. Kerherve, and J. Kirschner
Max-Planck Institut für Mikrostrukturphysik, Weinberg 2, 06120 Halle, Germany
(Received 2 November 2005; revised manuscript received 23 December 2005; published 26 January 2006)

Electronic correlations are manifested in many-body effects like superconductivity and magnetism. Established theoretical concepts show that the Coulomb and exchange interaction result in a tendency of two electrons to avoid each other, leading to an exchange-correlation (xc) hole. We will report on double photoemission (DPE) experiments using a time-of-flight setup consisting of a small central collector surrounded by a resistive anode. The first allows detection only within a narrow solid angle, therefore fixing the momentum. The resistive anode covers a solid angle of ~1 sr, the determination of the impact position results in momentum resolution. As a pulsed light source we used synchrotron radiation and we studied a NaCl(100) surface upon excitation with 34 eV photons. The very existence of coincidences is already a manifestation of the correlation. The onset of pair emission occurs when energy conservation allows the ejection of two electrons from the highest occupied level. We have made two key observations. If E_1 and E_2 are fixed such that a pair emission from the top of the valence band is possible, a zone of reduced intensity with a diameter of ~1.1 $Å^{-1}$ is visible. Recent calculations on DPE from a Cu(100) surface display exactly such a feature due to the xc hole. Hence we prove experimentally the very existence of the xc hole in double photoemission. The zone of reduced intensity disappears whenever emission below the top of the valence band becomes possible, indicating the sensitivity of the xc hole to inelastic scattering.

DOI: 10.1103/PhysRevB.73.041404 PACS number(s): 79.60.Bm

I. INTRODUCTION

Electrons in solids constitute a strongly interacting system and the description via independent particles ought to fail. However, Landau introduced the concept of quasiparticles.[1] It is in essence a transformation of the strongly interacting electron system to weakly interacting particles (quasiparticles) that still carry the spin and charge of an electron, albeit a renormalized mass. This concept may be understood in the context of screening. Intuitively it is clear that two electrons tend to avoid each other. First, the Coulomb interaction makes it energetically unfavorable for electrons to be close to each other. Second, the Pauli principle demands that electrons with parallel spin cannot be at the same location. Averaging over both spin directions still gives a reduced probability of finding two electrons at the same location. A more elaborate theoretical treatment for solids confirms this picture, and a pair correlation $\mathbf{g}(\mathbf{r},\mathbf{r}')$ function can be introduced.[2] This function describes the probability to find an electron at coordinates $\mathbf{r}$ when a second is located at $\mathbf{r}'$. The key result is that $\mathbf{g}$ is essentially constant (usually normalized to 1) except for small distances $|\mathbf{r}-\mathbf{r}'|<$ a few Å where $\mathbf{g}$ adopts smaller values. The spatial extent of this region is called the exchange-correlation (xc) hole and describes the length scale over which the correlation between electrons is relevant. This result can be rephrased by saying that each selected electron is surrounded by a positive charge exactly compensating for the electrons' charge. This feature is reminiscent of the screening of the Coulomb potential in solids. Hence, if the average distance between electrons is larger than the diameter of the xc hole they can be regarded as noninteracting particles and the description using independent-particle theories is appropriate.

Despite the fundamental importance of the concept of the xc hole, not much is known experimentally about the size and material dependence of the xc hole. A technique capable of studying the correlation between electron pairs is electron coincidence spectroscopy, where the excitation is due to electrons or photons [either termed $(e,2e)$ or $(\gamma,2e)$].[3–7] In fact, a recent publication theorized that k mapping of the double photoelectron emission (DPE) intensity opens an avenue of imaging the xc hole.[8] We will discuss our results obtained by DPE on a NaCl(100) surface that prove the existence of the xc hole and provide experimental determination of its spatial extent.

II. EXPERIMENT

Our experiments were conducted under UHV conditions featuring a time-of-flight spectrometer depicted in Fig. 1. The sample was a NaCl(100) surface that was kept at a temperature of ~100 °C. This temperature is sufficient to prevent charging up of the sample as evidenced by single electron spectra. The incident light hits the sample with an angle ~80° with respect to the surface normal. As a pulsed light source the BESSY II storage ring operating in the single bunch mode was employed, and the photon energy was fixed to 34 eV. In order to detect an electron pair, two detectors are required. A central collector accepts electrons only within a solid angle of ~0.02 sr, the detected electron we may term as the "fixed electron." A resistive anode[9] serves as the second detector which allows for a spatial resolution of the impact position.[10] Electrons within a solid angle of ~1 sr are registered, and we term them "free electrons". It is exactly this feature that constitutes the major experimental advance. The time differences between a photonbunch marker signal from the synchrotron and the fast-timing signals from the detectors were determined via time-to-amplitude converters in a coincidence circuit. With knowledge of the flight times

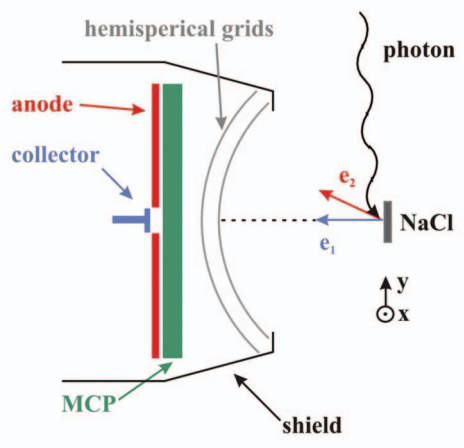

FIG. 1. (Color) Electron pair detection technique. Two electrons with momenta $\mathbf{k}_1,\mathbf{k}_2$ and energies E_1 and E_2 are detected in coincidence by a resistive anode and central collector.

of an electron pair the energies E_1,E_2 can be calculated. The total time resolution achieved in both channels was about 1 ns, while the energy resolution of the detected electrons depends on the particular energy value. For the electron energies discussed here the energy resolution amounts to ~0.5 eV. The impact position on the resistive anode determines the direction of $\mathbf{k}_1$ within a solid angle of ~1 sr except for the center, which is occupied by the central collector. The small collector in turn fixes the direction of $\mathbf{k}_1$. In this way we map out the energy and momentum dependence of the electron pair correlation. The experimental momentum resolution is 0.1 $Å^{-1}$. For all experiments the sample normal was pointing towards the central collector. This means that electrons reaching the central collector have an in-plane momentum of $|k_\parallel|<0.1$ $Å^{-1}$. The low coincidence count rate required a data acquisition time of 10 days.

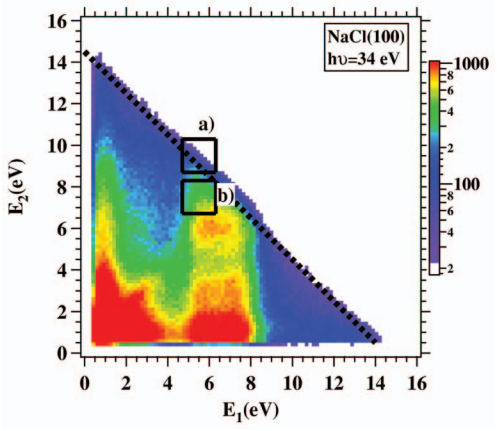

FIG. 2. (Color) The 2D energy distribution of coincidence electron pairs from a NaCl(100) surface is plotted. The photon energy was 34 eV. The energy E_1 (E_2) refers to the fixed electron (free electron). The dashed diagonal line marks the onset of pair emission, which occurs for a sum energy of ~14.6 eV. The square boxes labeled (a) and (b) indicate the events used to generate the 2-D momentum plots displayed in Fig. 3.

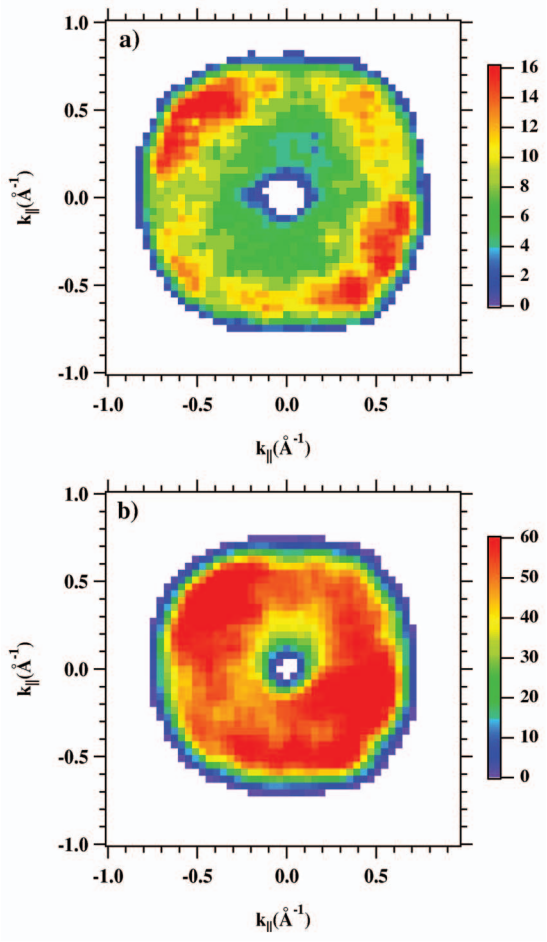

FIG. 3. (Color) The 2D in-plane momentum distribution for two different energy pairs from a NaCl(100) surface. In panel (a) we have selected E_1=5.5 eV and E_2=9.5 eV, whereas in panel (b) we have chosen E_1=5.5 eV and E_2=7.5 eV, respectively.

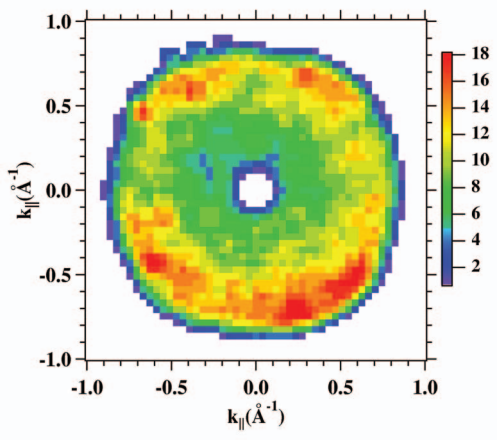

FIG. 4. (Color) The 2D in-plane momentum distribution as in Fig. 3 but for a LiF(100) surface excited with 30.7 eV electrons. The energies are E_1=7.5 eV and E_2=9.5 eV, respectively.

III. RESULTS

In Fig. 2 we plotted the 2D energy distribution of coincidence of electron pairs upon excitation with 34 eV photons. The energy of the fixed electron is labeled E_1 whereas that of the free electron is labeled E_2. We observe the onset of DPE when the sum energy E_1+E_2 equals ~14.6 eV. This is indicated by the dashed diagonal line in Fig. 2. This can be easily understood when considering the known binding energies of NaCl as determined by photoemission.[11] Wertheim *et al.* found that the highest occupied level (Cl 3*p* band) has a binding energy of $E_B=9.66$ eV with respect to the vacuum level.[11] Since for DPE two electrons leave the solid, this energy needs to be accounted for twice and subtracting this value from the photon energy yields the maximum kinetic sum energy

$$E_1 + E_2 = h\nu - 2E_B. \quad (1)$$

The numerical result is 14.68 eV and is in agreement with our observation. The very existence of a DPE intensity already implies the existence of correlation within the electron pair. This is a key result of a recent calculation by Berakdar.[12] The two-dimensional (2D) energy distribution shows a preferred emission of the fixed electron with energies of 6–8 eV, which is not present for the free electron.

More insight can be obtained if we take advantage of the lateral resolution of the setup. As a first step we select only those coincidences for which the energies E_1 and E_2 are fixed. In other words, we pick a point in the 2D energy distribution shown in Fig. 2. In order to obtain sufficient statistics we actually select an energy window of ±0.8 eV around the respective energies. This has been indicated by the square boxes in Fig. 2 labeled (a) and (b). We can now proceed and plot the coincidence intensity as a function of the in-plane momentum $k_\parallel$ of the free electron. We have selected two different regimes within the 2D energy distribution highlighted in Fig. 2 by the black squares. In case (a) we are right at the onset of pair emission. Case (b) describes the situation if emission below the highest occupied level is possible. In Fig. 3 we display the resulting momentum distributions. We would like to point out that all momentum plots display a zero intensity at a position where the central collector is positioned. The position and size of this blind spot depend on the momentum of the free electron. For the plots shown in Fig. 3 this blind spot is centered at $k_\parallel=0$ and has a radius of ~0.1 Å^{-1}. In Fig. 3(a) the energies are $E_1=5.5$ eV and $E_2=9.5$ eV [region (a) in Fig. 2]. We clearly observe that the region $k_\parallel=0$ (outside the blind spot) is surrounded by a region of diminished intensity. The intensity increases for larger $k_\parallel$ values and reaches a maximum for $k_\parallel \sim 0.55$ Å^{-1} and then falls off rapidly towards the edge of the channelplate. A dramatically different situation is depicted in Fig. 3(b) where we select $E_1=5.5$ eV and $E_1=7.5$ eV. Now the ring of enhanced intensity is essentially gone. Energetically the sum energy E_1+E_2 has been reduced from 15 eV to 13 eV. This energy difference allows for emission of a deeper-laying valence band electron or inelastic scattering losses if the electrons originate from the top of the valence band. Our results demonstrate the importance of inelastic scattering, which is very effective in destroying the hole shown in Fig. 3(a).

We may summarize our observations as follows: (i) If we select the energies E_1 and E_2 such that the sum energy E_1+E_2 has the largest possible value for pair emissions the 2D momentum plots display a region of reduced intensity that is centered around the fixed electron. (ii) If the sum energy is below the maximum value, a more or less uniform momentum distribution is the result.

IV. DISCUSSION

As we stated in the introduction, we expect each electron to be surrounded by an xc hole. It can be easily shown within the dipole approximation that a product of a single particle wave function yields a zero DPE intensity. However, due to the correlation/interaction such a product of wave functions is not correct and a nonzero DPE intensity results when going beyond the single-particle picture.[12] Therefore we can explain the momentum distribution in Fig. 3(a) as a consequence of the xc hole.

Such a notion is corroborated by the more thorough calculation by Fominykh *et al.* on the double photoemission of Cu(100).[8] They computed the in-plane momentum distribution (of the free electron) similarly to the plots shown in Fig. 3 for a photon energy of 42 eV and found that it exhibits a reduced intensity until $k_\parallel$ adopts a value of ~1.4 Å^{-1}. At this point the intensity rises sharply by roughly an order of magnitude. Shortly thereafter the intensity quickly returns to a small value. The ring of enhanced intensity has a diameter of 2.8 Å^{-1} and a width of ~0.2 Å^{-1}. The important outcome of the theoretical work is that the reduced intensity is a manifestation of the xc hole. Further, it was found that the DPE intensity also displayed the crystallographic symmetry of the surface. For NaCl we find the diameter of the reduced intensity region to be ~1.1 Å^{-1} if the energy of the free electron is 9.5 eV, and this diameter is significantly smaller than the theoretical value for Cu. Whether this difference is due to a comparison between different materials (noble metal versus insulator) is not clear. In that case we may take this as a hint of a material dependence. We emphasize that the size of the xc hole has been determined from the diameter of the maximum-intensity ring, which is near the edge of the detector, hence it is possible that the ring is even larger. This view is supported by the observation that the diameter increases with the increasing energy E_2 of the free electron (from 0.9 to 1.3 Å^{-1} for 7.5 to 13 eV) because the covered momentum space of the detector becomes larger. According to theory the xc hole shrinks if E_2 is increased.[8] Nevertheless, our key observation of a region of reduced intensity due to the xc hole remains valid and we quote the value for $E_2=9.5$ eV. In this context we would like to point out that we have performed a similar series of experiments on a LiF(100) surface, albeit excited by a primary electron gun.[13] As an example of the resulting momentum distributions we display in Fig. 4 the situation for a primary energy of 30.7 eV. The energies E_1 and E_2 are 7.5 eV and 9.5 eV, respectively. With this selection the sum energy has the highest possible value and only pair emission without any inelastic scattering of the pair

is possible. Further, we have chosen the same value of E_2 as that used in Fig. 3(a) in order to facilitate direct comparison. We immediately notice that there is no qualitative difference between Figs. 3(a) and 4. The study on LiF also showed that inelastic scattering destroys the region of reduced intensity similar to the plot in Fig. 3(b). Although two different materials have been studied (NaCl versus LiF) their electronic properties are very similar. Hence, we conclude that DPE [or $(\gamma,2e)$] and $(e,2e)$ experiments give qualitatively similar results despite the fact that the underlying mechanisms bear some significant differences. This point deserves further comment. The calculation of Fominykh *et al.*[8] did include only those contributions to the intensity where two electrons are ejected simultaneously upon absorption of a single photon. Energetically single photoemission is also possible whereby the excited electron may be regarded as a primary electron of an internal (e,2e) process. Experimentally we cannot discriminate between these two channels. The question arises what fraction these individual contributions make to the total DPE intensity. A hint is given by another theoretical study of Fominykh *et al.*[14] There they calculated the DPE intensity for Cu(100) and Ni(100) surfaces as a function of E_1-E_2 while keeping the sum energy E_1+E_2 constant at the highest value possible (pair emission from E_F). They showed that for Cu(100) the internal $(e,2e)$ process is much less efficient compared to that for the Ni(100) surface, due to the higher density of states (DOS) at E_F for Ni.[8] From this study we learn that the contribution of the internal $(e,2e)$ process does depend on the system. As far as NaCl and LiF are concerned, we are not aware of a theoretical study dealing with this aspect and hence we cannot comment on the significance of this contribution to the total DPE intensity. Nevertheless we conclude from our work that we have mapped the xc hole via DPE. In contrast to theory we were not able to resolve the crystallographic symmetry, which may be due to insufficient statistics. An aspect not treated theoretically so far is the sensitivity of the xc hole on inelastic scattering, which is very effective in suppressing the emergence of the xc hole as this study shows.

V. SUMMARY

We have shown that with momentum mapping of the DPE intensity imaging of the xc hole is possible. We have determined the diameter of the xc hole to be ~ 1.1 Å^{-1} (for $E_2 = 9.5$ eV) for a NaCl(100) surface. Qualitatively similar results can be achieved if a pulsed electron gun is used. A larger angular acceptance would ultimately allow us to study the material dependence of the xc hole. In order to disentangle the exchange from the Coulomb part, experiments on ferromagnetic surfaces with photons of different helicities appear to be promising.

ACKNOWLEDGMENT

We thank the staff of the BESSY II storage ring for the excellent support.

[1] L. D. Landau, Sov. Phys. JETP **3**, 920 (1957).
[2] P. Fulde, *Electron Correlations in Molecules and Solids*, Springer Series in Solid State Sciences Vol. 100 (Springer, Berlin, 1993).
[3] H. W. Biester, M. J. Besnard, G. Dujardin, L. Hellner, and E. E. Koch, Phys. Rev. Lett. **59**, 1277 (1987).
[4] J. Kirschner, O. M. Artamonov, and S. N. Samarin, Phys. Rev. Lett. **75**, 2424 (1995).
[5] S. Iacobucci, L. Marassi, R. Camilloni, S. Nannarone, and G. Stefani, Phys. Rev. B **51**, R10252 (1995).
[6] A. Morozov, J. Berakdar, S. N. Samarin, F. U. Hillebrecht, and J. Kirschner, Phys. Rev. B **65**, 104425 (2002).
[7] R. Herrmann, S. Samarin, H. Schwabe, and J. Kirschner, Phys. Rev. Lett. **81**, 2148 (1998).
[8] N. Fominykh, J. Berakdar, J. Henk, and P. Bruno, Phys. Rev. Lett. **89**, 086402 (2002).
[9] Quantar Technology Incorporated, Model 3300 SERIES MCP.
[10] S. N. Samarin, O. M. Artamonov, D. K. Waterhouse, J. Kirschner, A. Morozov, and J. F. Williams, Rev. Sci. Instrum. **74**, 1274 (2003).
[11] G. K. Wertheim, J. E. Rowe, D. N. E. Buchanan, and P. H. Citrin, Phys. Rev. B **51**, 13675 (1995).
[12] J. Berakdar, Phys. Rev. B **58**, 9808 (1998).
[13] F. O. Schumann, J. Kirschner, and J. Berakdar, Phys. Rev. Lett. **95**, 117601 (2005).
[14] N. Fominykh, J. Berakdar, J. Henk, S. Samarin, A. Morozov, F. U. Hillebrecht, J. Kirschner, and P. Bruno, *Solid-State Photoemission and Related Methods* (Wiley-VCH, Weinheim, 2003)